

## Supporting Information

### Enhanced photoluminescence stability and internal defect evolution of the all-inorganic lead-free CsEuCl<sub>3</sub> perovskite nanocrystals

#### 1. PL stability of the uncoated CsEuCl<sub>3</sub> nanocrystals

The gradually enhanced emissions were observed during the first 5 days. The emission decreased after 5 days, and the remnant PL reduced to about 20 % of the initial value at the 10th day. Moreover, a rapidly decomposed occurred while the pure CsEuCl<sub>3</sub> nanocrystal exposed to ambient atmosphere.

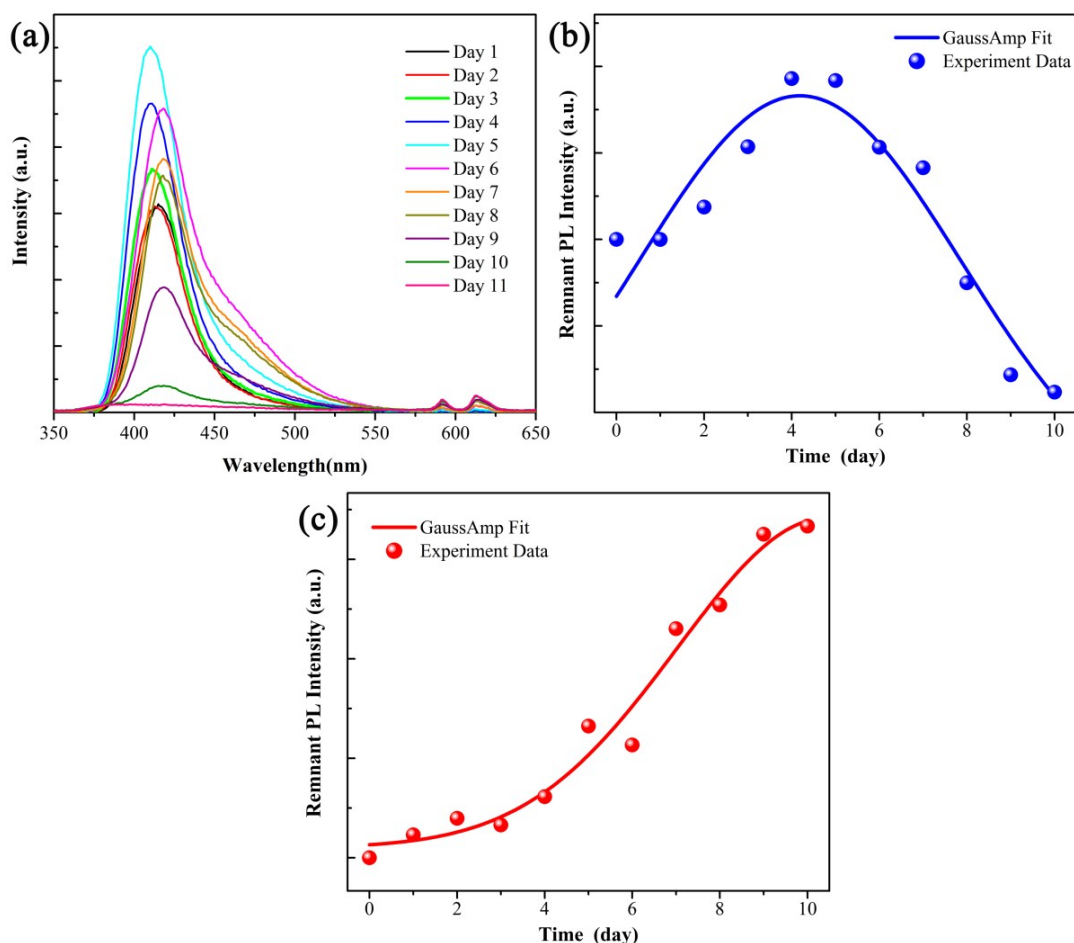


Figure S1 (a) The fluorescence varies with time, (d) the residual blue emission intensity, and (c) the residual red emission intensity of the uncoated CsEuCl<sub>3</sub> nanocrystals.

## 2. XRD characterization of the unmodified CsEuCl<sub>3</sub> perovskite nanocrystals

The CsEuCl<sub>3</sub> nanocrystals thin film was spin-coated on a quartz substrate at 3000 rpm for 60s in the glove box, and then the sample was sealed in a centrifuge tube. The XRD characterization and digital images of the luminescence were performed immediately when the sample removed from the glove box. Fig.S2a shows the obtained XRD pattern of the sample, the result revealing that the sample was suffer from destruction. Fig.S2b show the luminescence images of the sample exposed in environment. Apparently, the luminescence is extremely unstable and sensitive to the environment. Thus, it can be predicted that the CsEuCl<sub>3</sub> nanocrystals is very hard to perform the further physical characteristic analysis and practical application under nonspecial conditions.

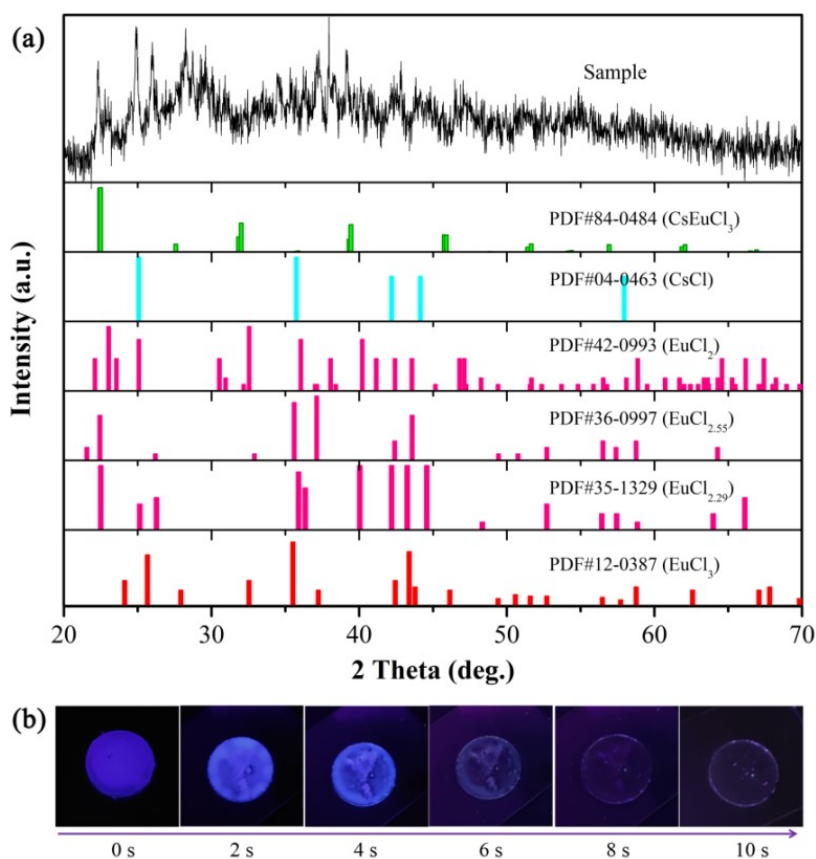


Fig. S2 (a) The XRD pattern and (b) digital luminescence images of the unmodified sample.

### 3. Size distribution

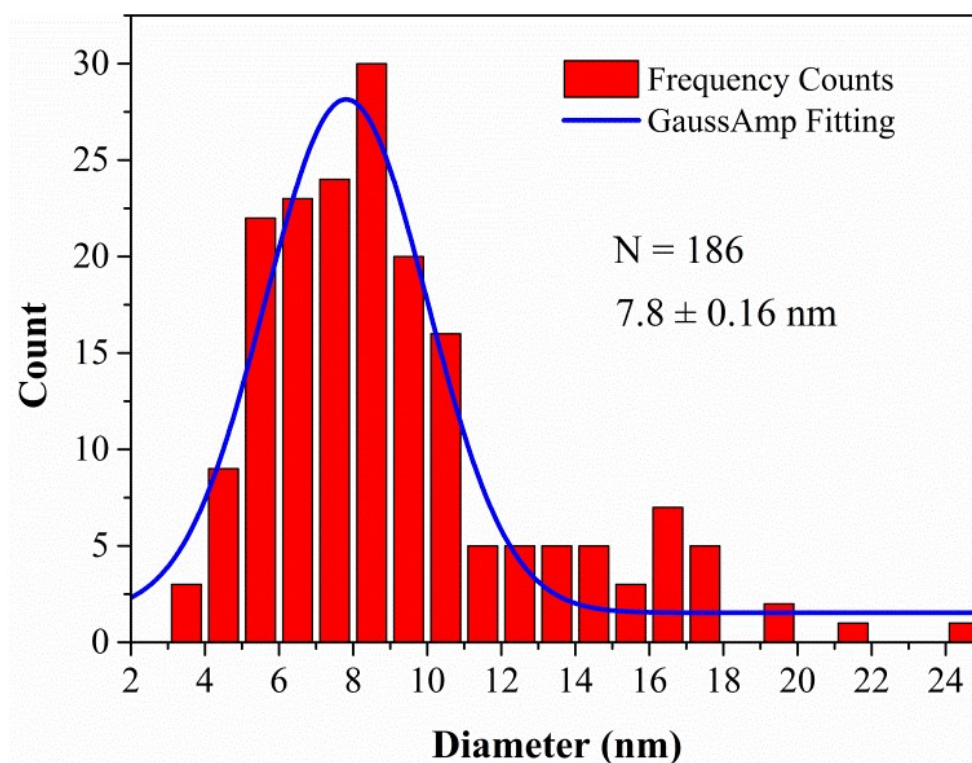


Fig. S3 The size distribution of CsEuCl<sub>3</sub> nanocrystals.

### 4. Residual red emission intensity of the silica-coated CsEuCl<sub>3</sub> nanocrystals

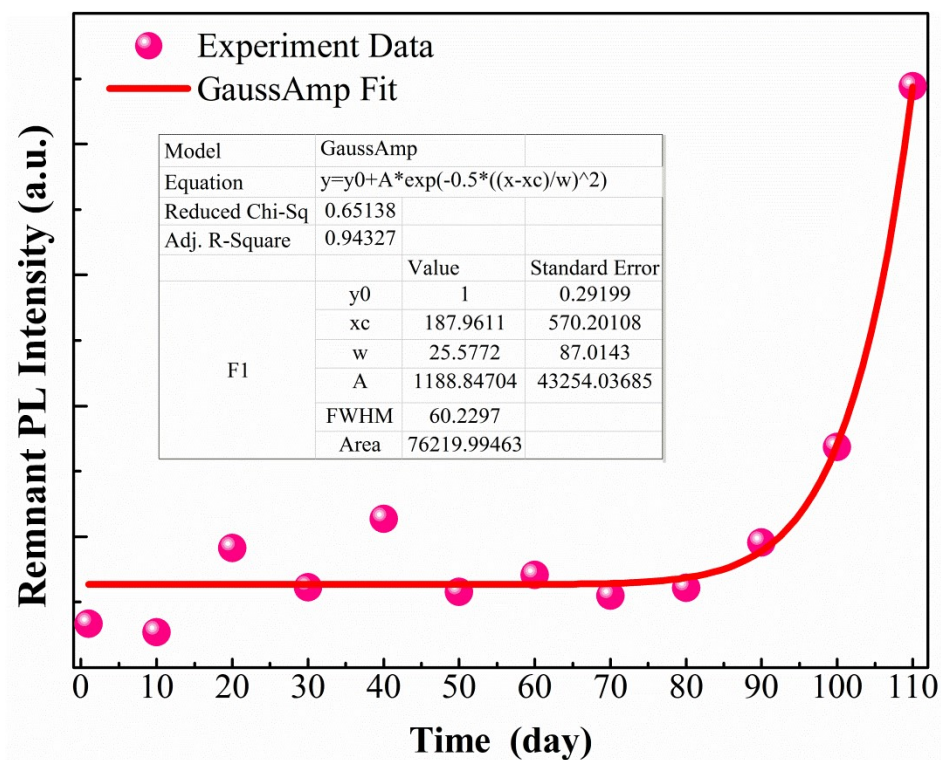


Fig. S4 The residual red emission intensity of the silica-coated CsEuCl<sub>3</sub> nanocrystals.

## 5. Electronic band structure calculation models

The cutoff energy for the plane-wave basis set was set to 500 eV. The DFT+U method was applied using 2.5 eV Hubbard U value for the *d* orbital of Eu. A 3×3×3 CsEuCl<sub>3</sub> supercell was used, and the vacancy-CsEuCl<sub>3</sub> was simulated by removing two CsEuCl<sub>3</sub> units from the same supercell. The geometry optimizations were performed until the forces on each ion were reduced below 0.01 eV/Å, and the 2×2×2 K-point sampling of the Brillouin zone was used.

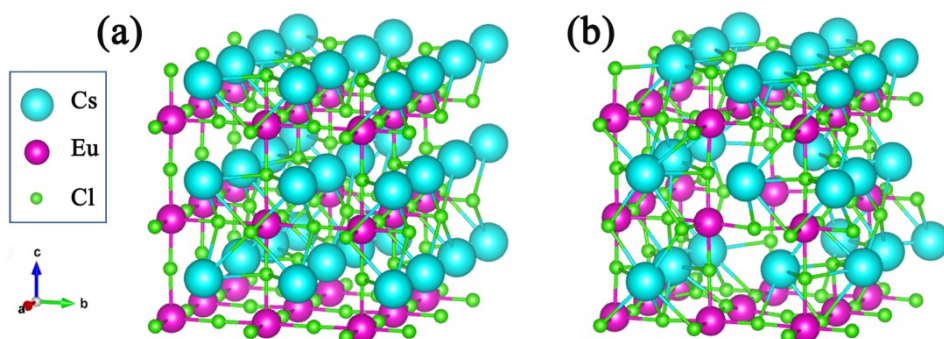


Fig. S5 Structural derivation of the  $V_{Eu}$  and “hollow” lattices from the proper 3D perovskite.

## 6. XRD characterization of the silica-coated CsEuCl<sub>3</sub> nanocrystals

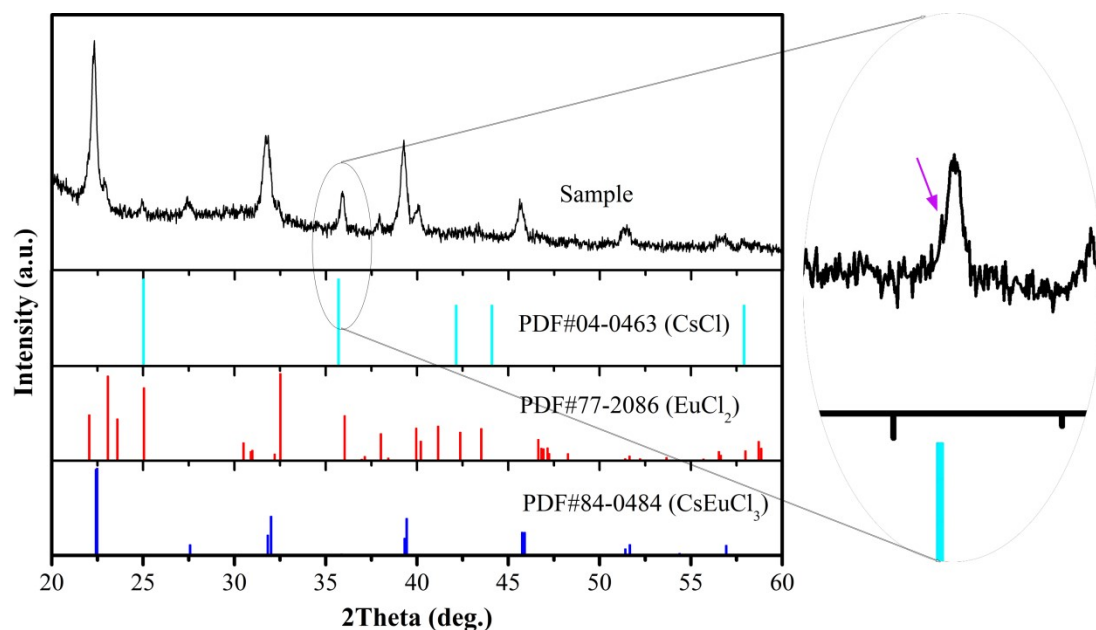


Fig. S6 XRD pattern of silica-coated CsEuCl<sub>3</sub> nanocrystals after stored 80 days

## 7. Calculated energy band information

**Table S1** Calculated energy band information of the CsEuCl<sub>3</sub> supercell.

<b>Spin Channel</b>		<b>Up</b>	<b>Down</b>	<b>Total</b>
<b>Model 1</b>	Band gap	2.9677	5.2310	2.9677
<b>(V<sub>Eu</sub>)</b>	Eigenvalue of VBM	1.0971	-1.1074	1.0971
	Eigenvalue of CBM	4.0648	4.1236	4.0648
	Fermi Energy	1.3186	1.3186	1.3186
	HOMO Band	27	20	27
	LUMO Band	28	21	28
<b>Model 2</b>	Band gap	3.0734	5.1066	3.0734
<b>(Hollow)</b>	Eigenvalue of VBM	0.8767	-1.0918	0.8767
	Eigenvalue of CBM	3.9500	4.0149	3.9500
	Fermi Energy	1.1121	1.1121	1.1121
	HOMO Band	27	20	27
	LUMO Band	28	21	28